Final Draft
of the original manuscript:

Zerbst, U.; Pempe, A.; Scheider, I.; Ainsworth, R.A.; Schoenfeld, W.:
Proposed extension of the SINTAP/FITNET thin wall option based on a simple method for reference load determination
In: Engineering Fracture Mechanics (2008) Elsevier

DOI: 10.1016/j.engfracmech.2008.06.029

PROPOSED EXTENSION OF THE SINTAP THIN WALL OPTION BASED ON A SIMPLE METHOD FOR REFERENCE LOAD DETERMINATION

Zerbst, U.[a], Pempe, A.[a], Scheider, I.[a], Ainsworth, R.A.[b], Schönfeld, W.[a]

[a] GKSS Research Centre, Institute for Materials Research, Materials Mechanics, D-21502 Geesthacht, Germany

[b] British Energy Generation Limited, Barnwood, Gloucester GL4 3RS, UK

ABSTRACT

A "correct" limit or yield load is an essential element of flaw assessment procedures of the R6 or SINTAP type. In the present paper the authors propose a definition of this quantity which is based on the SINTAP Option 3 failure assessment function. This "reference load" can be determined for any component geometry by finite element analyses. The method is applied to two kinds of thin walled structures (notched plates and curved stiffened panels) this way extending the existing thin wall module of SINTAP.

Key words

Flaw assessment, R6 procedure, SINTAP, FITNET, stable crack extension, thin walled structures, reference load, CTOD-δ_5.

1. INTRODUCTION

2. THE SINTAP THIN WALL OPTION OF FITNET

In [1] and [2] the authors proposed a thin wall module of the European flaw assessment procedure SINTAP which then became part of the extended assessment procedure developed in the FITNET project [3]. For a detailed description of the module see also Section 6.10 in [4]. The module uses the basic equations of SINTAP but in conjunction with the CTOD-δ_5 concept (**Figure 1**) [5], so that the elastic-plastic opening over a 5mm gauge length, δ_{5ep}, is related to the elastic value δ_{5e} by:

$$\delta_{5ep} = \delta_{5e} \cdot f\left(L_r\right)^{-2} \tag{1}$$

$$\delta_{5e} = \frac{K^2}{m \cdot E' \cdot \sigma_Y} \tag{2}$$

with both the effective Young's modulus, E' and the constraint parameter m being defined for plane stress conditions as Young's modulus E and unity, respectively. The ligament yielding parameter L_r is defined by

$$L_r = F/F_Y = \sigma_{ref}/\sigma_Y \tag{3}$$

with F being the applied load, F_Y the plastic limit load (in [4] designated as yield load) of the cracked component, σ_Y the yield strength of the material and σ_{ref} a reference stress of the cracked component defined by Eqn. (3).

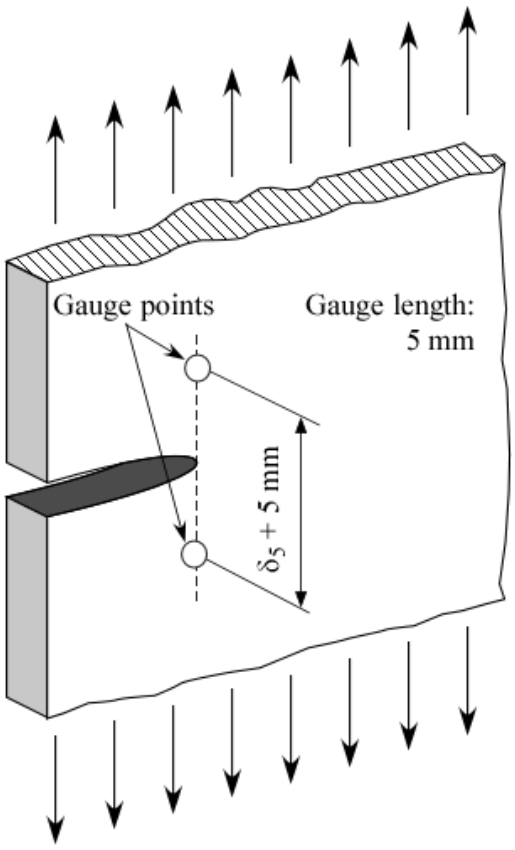

Figure 1: Definition of the crack tip opening displacement CTOD-δ_5.

The function $f(L_r)$ is defined for different analysis levels. Within the present paper only the Option 3 (stress-strain based option) function in SINTAP (see [4]; note this is termed Option 2 in the R6 procedure [6]) is applied. For this the $f(L_r)$ function is given by

$$f(L_r) = \left[\frac{E \cdot \varepsilon_{ref}}{\sigma_{ref}} + \frac{1}{2} \frac{L_r^2}{E \cdot \varepsilon_{ref}/\sigma_{ref}} \right]^{-1/2} \quad \text{for } 0 \le L_r \le L_r^{max} \tag{4}$$

and

$$L_r^{max} = 0.5 \cdot \left[(\sigma_Y + R_m)/R_{eL} \right]. \tag{5}$$

where R_m is the ultimate tensile strength and ε_{ref} is the total strain from the uniaxial stress-strain curve at the stress σ_{ref}. From Eqn. (3) the reference stress σ_{ref} is related to the ligament yielding parameter L_r by

$$\sigma_{ref} = L_r \cdot \sigma_Y \,. \tag{6}$$

This then defines the corresponding reference strain ε_{ref} on the true stress-stain curve as illustrated in **Figure 2**. The application of Option 3 requires stress-strain curves of relatively high quality. In particular the yield strength region should be adequately represented including data points at least at L_r = 0.7, 0.9, 0.98, 1.00, 1.02, 1.10 and 1.20.

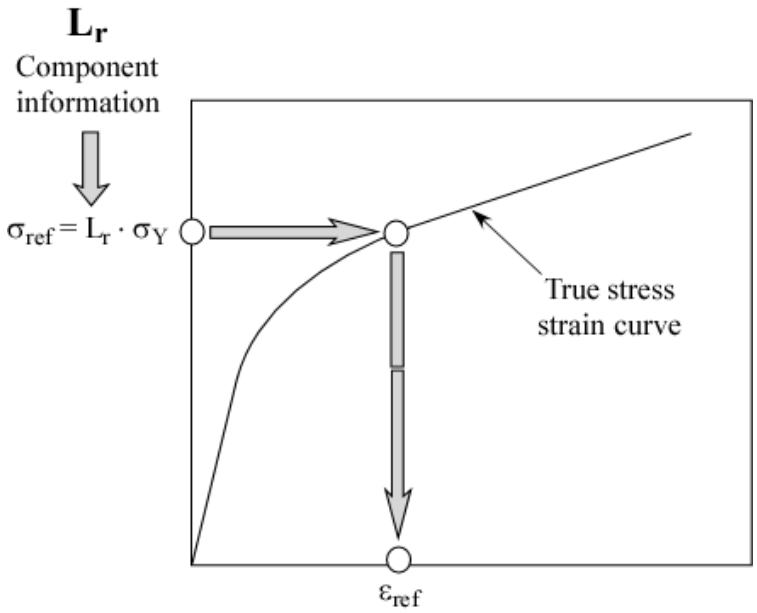

Figure 2: SINTAP (FITNET) Option 3: Determination of (σ_{ref},ε_{ref}) points on the true stress-strain curve dependent on the ligament yielding parameter L_r of the component.

Note that the δ_5 crack tip parameter besides the crack tip opening angle (CTOA) is also one of the two standard parameters for toughness determination under the low constraint conditions relevant to typical thin walled geometries [7, 8].

Usually the aim of a SINTAP thin wall analysis is the determination of the maximum load a structure can sustain considering stable crack extension. A schematic representation of how this can be performed is provided in **Figure 3**.

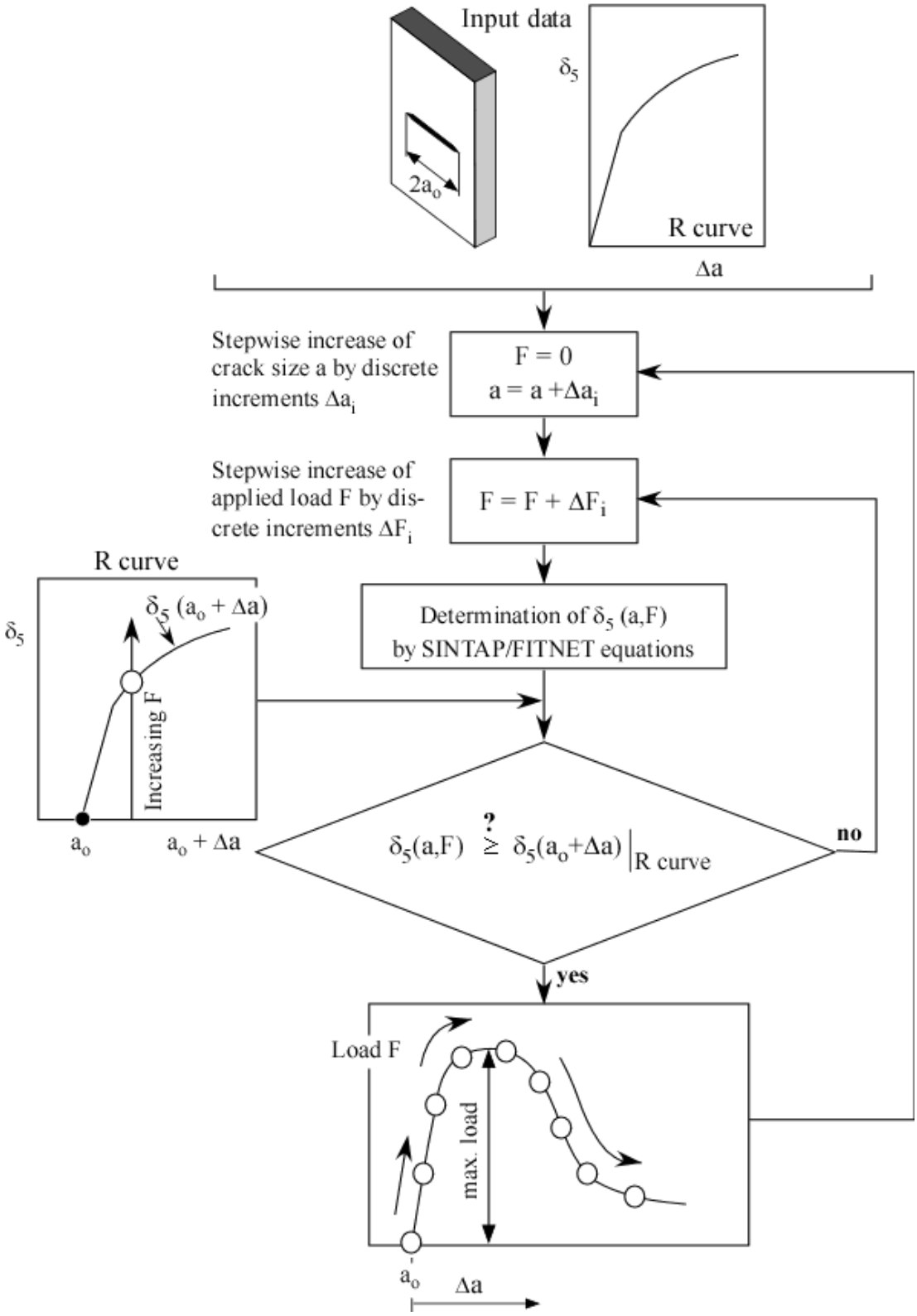

Figure 3: Flow chart for determining the maximum load a thin walled structure can sustain taking into account stable crack extension.

In addition to the use of the δ_5 concept and the consideration of stable crack extension the SINTAP (FITNET) thin wall module is characterised by further specific features. For example, it takes routinely into account potential anisotropy in tensile properties (thin plates are usually manufactured by rolling). The limitations of the assessment procedure are set by the δ_5 concept. With respect to the maximum stable crack extension these refer to

$$\Delta a_{max} = \begin{cases} 0.25\,(W - a_o) & C(T) \text{ and } SE(B) \text{ specimens} \\ W - a_o - B & M(T) \text{ specimens} \end{cases} \tag{7}$$

In order to avoid extrapolation of the δ_5-Δa curve beyond its validity limits the predicted stable crack extension Δa at the maximum load in the component should not exceed the Δa range which is covered by the experimental R-curve.

The δ_5-R-curve has to be obtained on specimens of thickness, B, identical to the component and a crack length, a_o, and an initial uncracked ligament length, W- a_o, equal to or greater than four times the thickness, B.

$$a_o / B \text{ and } (W - a_o) / B \geq 4 \tag{8}$$

It has been shown [9, 10] that R-curves of aluminium alloys tend to be independent of the specimen geometry and dimensions when these requirements are fulfilled. However, this statement cannot be generalised for any material and any case. In cases where no geometry independency is stated the lowest R-curve has to be used which is usually obtained from bend specimens.

The SINTAP thin wall module has successfully been validated for a large number of thin wall plates made of different aluminium alloys and steels, for uniaxial and biaxial tension loading and bending, and for Mode I and mixed mode crack extension ([1-2, 11], see also Section 7.3 in [4]). Note however that all these examples included simple plane geometries without stiffeners or notches which, however, are typical elements of thin walled structures. In the following sections an extension of the procedure to more complex structures is proposed and evaluated.

3. DETERMINATION OF THE REFERENCE LOAD F_Y

As mentioned above, one of the key parameters for any flaw assessment of the R6 or SINTAP type is the limit or yield load beyond which the ligament becomes fully plastic and the load-local displacement characteristics of the cracked structure becomes non-linear. An exact prediction of the load carrying capacity of a cracked component requires a “correct” limit load the provision of which, however, is not an easy task because the limit loads available in handbooks and compendia (among others [12-17]) have been obtained over decades by different methods and are of quite different quality. Much effort has been spent on the generation of improved limit load solutions particularly of plates and hollow cylinders with semi-elliptical surface cracks; these are not discussed here in detail but reference may be made to Section 5.2 in [4] for further details.

It should be noted that what is actually needed is not strictly a limit load but a reference load which is consistent with the flaw assessment model used. The idea of using the basic

equations of assessment models such as the EPRI handbook [18] or the R6 procedure [6] in conjunction with finite element results for the J-integral or CTOD to define such a reference load is not new. For example, a reference load, P_o, has been combined with the normalised (h) functions in the EPRI method [19] to define J; for details see [20-21]. The reference load has also been chosen so that fully plastic solutions for power-law materials (such as those in [19]) for different values of hardening exponent n are insensitive to n (Ainsworth [22], Kim et al. [23]). The ability to make power-law solutions insensitive to n has been used to justify use of classical limit load solutions as reference loads since these correspond to $n \rightarrow \infty$. Alternatively Eqns. (1) and (4), or corresponding J estimates, can be fitted over a range of loads (range of L_r) with the load F_Y chosen so that numerical CTOD or J results are well fitted. Recently, Kim et al. [24] and Lei [25] followed similar approaches for investigating limit load solutions of plates with semi-elliptical surface cracks.

In the present paper the authors adopt a simple but well-defined approach for defining the reference load F_Y from numerical results. When the applied load is equal to the reference load, $L_r = 1$ in the SINTAP $f(L_r)$ function of Eqn. (4). The reference stress σ_{ref} is then identical to the yield strength σ_Y and ε_{ref} is the corresponding strain (Figure 2). Depending only on the material stress-strain curve, the value of $f(L_r)$ is obtained for $L_r = 1$ from Eqn (4) and this in turn corresponds to a certain J/J_e ratio as

$$J_{ep}/J_e = f\left(L_r = 1\right)^{-2} \tag{9}$$

with J_{ep} being the elastic-plastic and J_e the elastic J-integral. The reference load F_Y then corresponds to that load at which Eqn.(9) is satisfied (**Figure 4**). Both J_{ep} and J_e can be determined for any geometry, e.g., by finite element analysis. In practice, the determination of the reference load is based on the J-integral and not on the CTOD-δ_5 (Eqn. 1) or other CTOD definitions since the $f(L_r)$ functions have originally been determined for J even though they are successfully used with δ_5 in the SINTAP thin wall module.

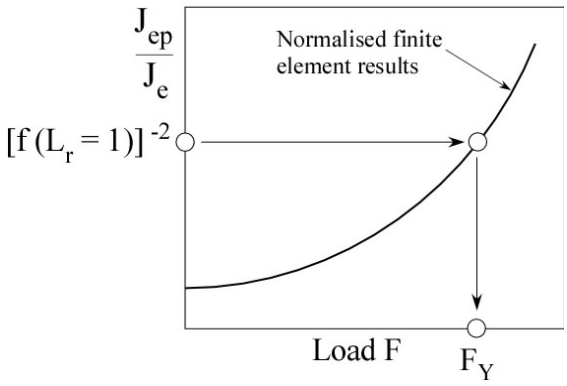

Figure 4: Principle for the determination of the reference load F_Y in the present paper.

The above approach for determination of F_Y could be based on any value of L_r rather than $L_r = 1$. However, at small L_r Eqn. (4) is relatively insensitive to L_r and $f(L_r)$ is approximately unity. At large L_r gross plastic yielding can make numerical determination of J difficult, the stress-strain curve can be flat making determination of ε_{ref} difficult, and large values of L_r are not relevant in practice. Therefore $L_r = 1$ is chosen as a value at which the effects of plasticity

are significant (typically $f(L_r = 1) = 0.6$ and $J_{ep}/J_e = 3$), determination of ε_{ref} is straightforward and results are relevant to practical load levels.

Once the reference load F_Y has been determined it can be applied with the SINTAP procedure to assess the structure under consideration. Of course, it does not make much sense to apply the analytical assessment method instead of the finite element results to the specific component made of the specific material with the crack for which the finite element analysis has been performed. However, there are many applications where the combination of numerical and analytical analysis steps is advantageous, for example, when the applied primary load acts in conjunction with secondary loads, such as welding residual stresses, for which numerical solutions do not exist; and to assess variations in material properties and temperatures from those for which the numerical analysis has been performed. The methodology can also be applied to generate new reference load solutions instead of the available limit load solutions. These should than allow better results than available at present. There are also many configurations for which no limit load solutions exist at all in handbook format. In the next two sections of this paper the proposed approach is applied to two kinds of structure.

4. APPLICATION TO THIN WALLED NOTCHED GEOMETRIES

The first example refers to notched thin walled plates the geometry of which is shown in **Figure 5** and summarised in **Table 1**. The stress-strain data of the materials used in the analyses are provided in **Figure 6** and **Table 2**.

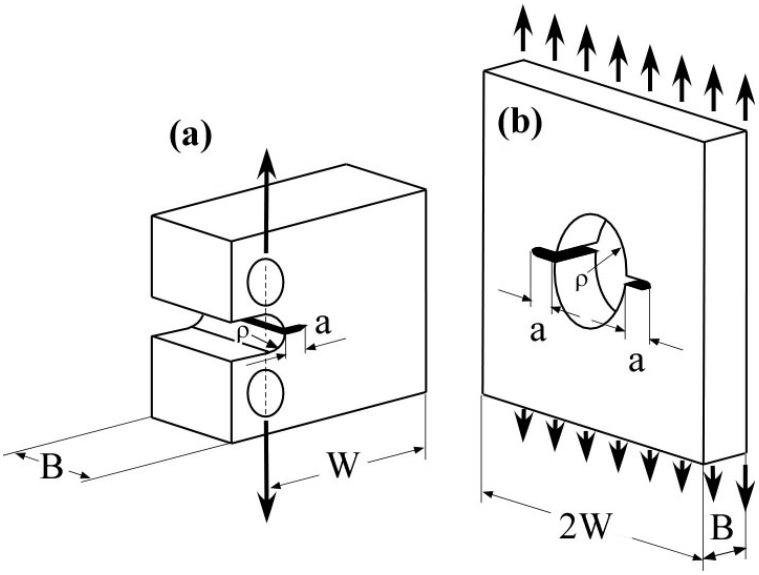

Figure 5: Basic geometries of the notched geometries investigated in Section 4.

Table 1: Notched geometries investigated in Section 4.

Material	Loading type	Specimen dimensions in mm	Notch radius ρ in mm	Crack depth a in mm	a/ρ ratio
35 NiCrMo16 (ferritic steel)	Tension (9 specimens)	B = 5 W = 100	3 / 9 / 15	1.5 / 3 / 4.5 / 6 / 7.5 / 9 / 15 / 18 / 30	0.5 / 1 / 2
35 NiCrMo16 (ferritic steel)	Tension + bending (9 specimens)	B = 5 W = 100	3 / 9 / 15	1.5 / 3 / 4.5 / 6 / 7.5 / 9 / 15 / 18 / 30	0.5 / 1 / 2
X6 CrNi 18 11 (austenitic steel)	Tension (9 specimens)	B = 10 W = 100	3 / 9 / 15	1.5 / 3 / 4.5 / 6 / 7.5 / 9 / 15 / 18 / 30	0.5 / 1 / 2
X6 CrNi 18 11 (austenitic steel)	Tension + bending (9 specimens)	B = 10 W = 100	3 / 9 / 15	1.5 / 3 / 4.5 / 6 / 7.5 / 9 / 15 / 18 / 30	0.5 / 1 / 2
Al 5083 H 321 (aluminium alloy)	Tension (9 specimens)	B = 3 W = 100	3 / 9 / 15	1.5 / 3 / 4.5 / 6 / 7.5 / 9 / 15 / 18 / 30	0.5 / 1 / 2
Al 5083 H 321 (aluminium alloy)	Tension + bending (9 specimens)	B = 3 W = 100	3 / 9 / 15	1.5 / 3 / 4.5 / 6 / 7.5 / 9 / 15 / 18 / 30	0.5 / 1 / 2

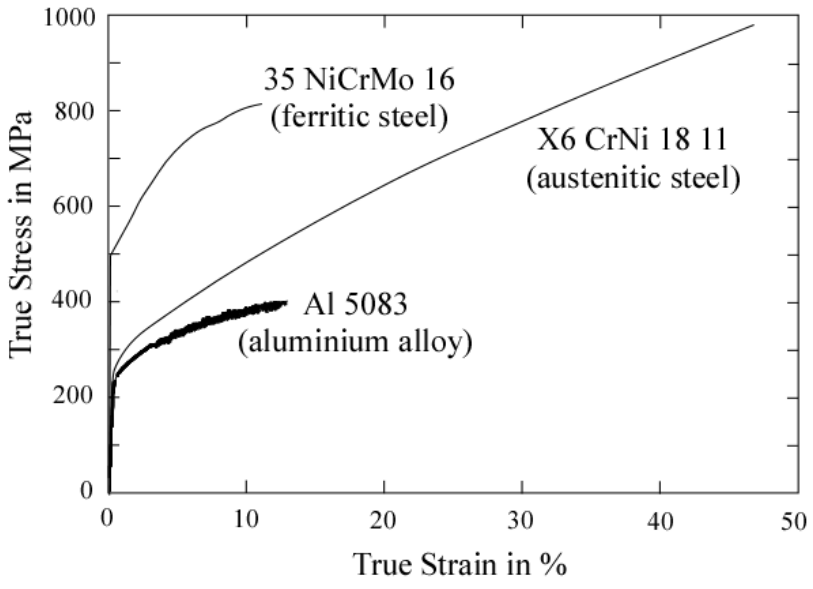

Figure 6: True stress-strain curves of the materials used for the simulations in Section 4.

Table 2: Tensile properties of the materials used for the simulations in Section 4.

Material	Young's Modulus E in GPa	Yield strength σ_Y [1)] in MPa	Ultimate tensile strength R_m in MPa
35 NiCrMo 16	215	510	726
X6 CrNi 18 11	195	240	617
Al 5083 H321	70.3	242	350

1) $\sigma_Y = R_{eL}$ for 35 NiCrMo 16; $\sigma_Y = R_{p0.2}$ for Al 5083 H321 and X6 CrNi 18 11.

For each of the 54 specimens investigated the stress intensity factor, K, as well as the reference load, F_Y, was determined by finite element analyses using the program ABAQUS [26]. All calculations were performed in plane stress in order to simulate thin wall conditions.

The reference load solutions can be expressed by

$$F_Y = 2\beta\left(W - a\right)B\sigma_Y \tag{10}$$

for the M(T) geometries (tension loading) and by

$$F_Y = \beta\left\{\left[\left(1+\gamma\right)\cdot\left(1+\gamma\cdot\left(a/W\right)^2\right)\right]^{1/2} - 1 - \left(\gamma a\right)/W\right\}WB\sigma_Y \tag{11}$$

for the C(T) geometries, under combined tension and bending loading according to

$$M = F\cdot\frac{W}{2} \tag{12}$$

with M being the bending moment and F the tensile force. Eqns. (10) and (11) refer to un-notched geometries (M(T) [13], C(T) [14]) but corrected by a notch factor β which is obtained from the present calculations and summarised in **Tables 3** and **4**.

Table 3: Notch correction factor β of the limit load solution for M(T) geometries (Eqn. 10), Section 4.

Material	σ_Y in MPa	ρ in mm	a in mm	a/ρ	β
		3	1.5	0.5	0.97
		3	3	1	0.98
		3	6	2	0.98
		9	4.5	0.5	1.01
35 NiCrMo 16	510	9	9	1	1.02
		9	18	2	1.02
		15	7.5	0.5	1.02
		15	15	1	1.03
		15	30	2	1.03
		3	1.5	0.5	0.90
		3	3	1	0.91
		3	6	2	0.92
		9	4.5	0.5	0.94
X6 CrNi 18 11	240	9	9	1	0.97
		9	18	2	1.00
		15	7.5	0.5	0.99
		15	15	1	1.02
		15	30	2	1.06
		3	1.5	0.5	0.92
		3	3	1	0.93
		3	6	2	0.94
		9	4.5	0.5	0.97
Al 5083 H321	242	9	9	1	0.99
		9	18	2	1.02
		15	7.5	0.5	1.00
		15	15	1	1.02
		15	30	2	1.04

Table 4: Notch correction factor β of the limit load solution for C(T) geometries (Eqn. 11), Section 4.

Material	σ_Y in MPa	ρ in mm	a in mm	a/ρ	β
		3	1.5	0.5	0.67
		3	3	1	0.71
		3	6	2	0.77
		9	4.5	0.5	0.83
35 NiCrMo 16	510	9	9	1	0.89
		9	18	2	0.94
		15	7.5	0.5	0.91
		15	15	1	0.94
		15	30	2	0.99
		3	1.5	0.5	0.86
		3	3	1	0.89
		3	6	2	0.96
		9	4.5	0.5	1.02
X6 CrNi 18 11	240	9	9	1	1.06
		9	18	2	1.12
		15	7.5	0.5	1.10
		15	15	1	1.11
		15	30	2	1.17
		3	1.5	0.5	0.76
		3	3	1	0.82
		3	6	2	0.87
		9	4.5	0.5	0.93
Al 5083 H321	242	9	9	1	0.98
		9	18	2	1.05
		15	7.5	0.5	1.02
		15	15	1	1.06
		15	30	2	1.06

The values of K and F_Y were then used to predict finite element based applied load versus δ_5 curves, some of which are shown in **Figures 7** to **9**. The cases reproduced represent limit conditions (smallest notch radius + smallest crack / largest notch radius + largest crack) for tension and combined tension/bending for all three materials. The quality of the 42 predictions (cf. Tables 3 and 4) not shown here are comparable or better than these examples.

Whilst the analyses of the austenitic steel and the aluminium alloy throughout show very satisfying results, i.e. the SINTAP predictions are close to the finite element curves the results obtained for the ferritic steel are of lower quality. Whilst the results are commonly conservative, i.e., SINTAP underestimates the load compared to the finite element curves there are some exceptions. At low load values SINTAP tends to slightly overestimate the load for given δ_5. The reason might be that the J-integral based $f(L_r)$ function is straightforward but

when applied to δ_5 the $\delta_{5e} \square K^2$ expression in Eqn. (2) is correct only in the upper contained yielding range. However, the resulting non-conservatism is fairly small.

In the fully plastic branches of the load versus δ_5 curves (beyond F_Y) all predictions for the austenitic steel and the aluminium alloy and most for the ferritic steel are moderately conservative. There are, however a few exceptions for the ferritic steel one of which is shown in Figure 7. Moderately non-conservative curves were predicted for M(T) geometries with small notch radii (ρ = 3 mm) and δ_5 values beyond about 0.2 mm or more (Figure 7, top-left).

Summarising, the application of the method proposed in Section 3 allowed reasonable predictions for the range of notch radii, crack sizes, loading geometries and materials investigated. The pure bending case was not investigated because it does not play any role in thin walled structures which in reality would fail by buckling rather than by bending.

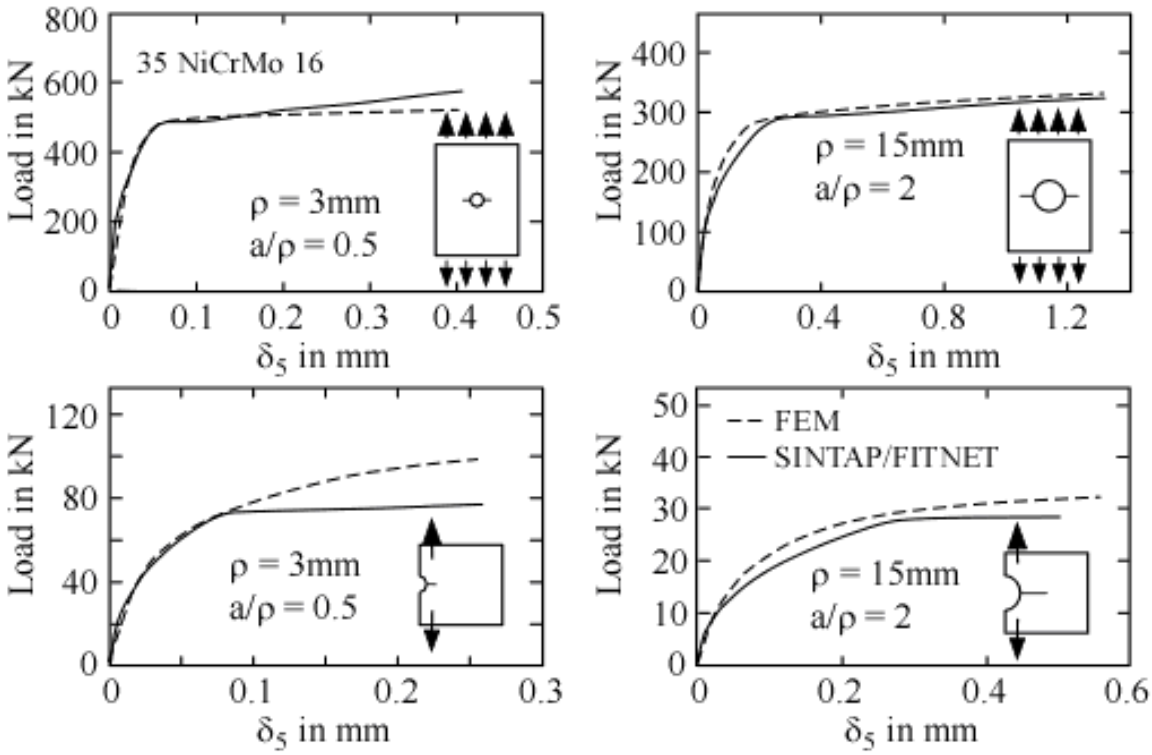

Figure 7: Comparison between the finite element and the modified SINTAP based load versus δ_5 characteristics for the ferritic steel 35 NiCrMo 16, Section 4.

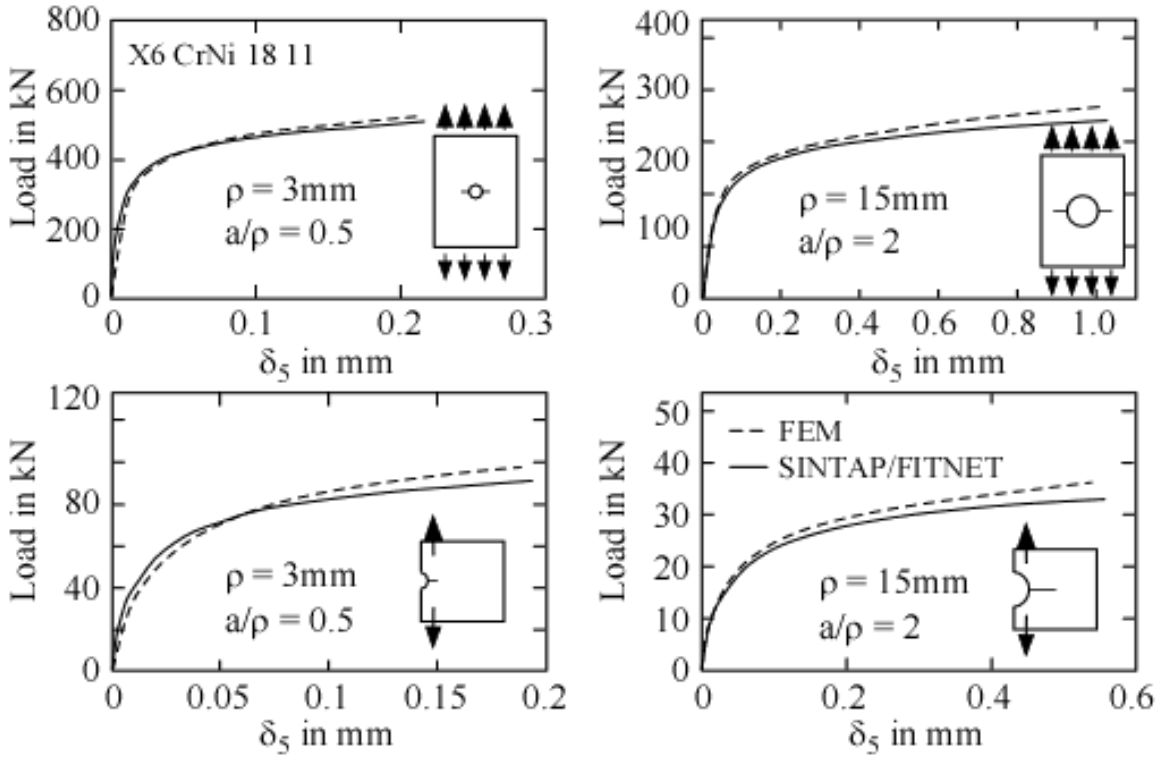

Figure 8: Comparison between the finite element and the modified SINTAP based load versus δ_5 characteristics for the austenitic steel X6 NiCr 18 11, Section 4.

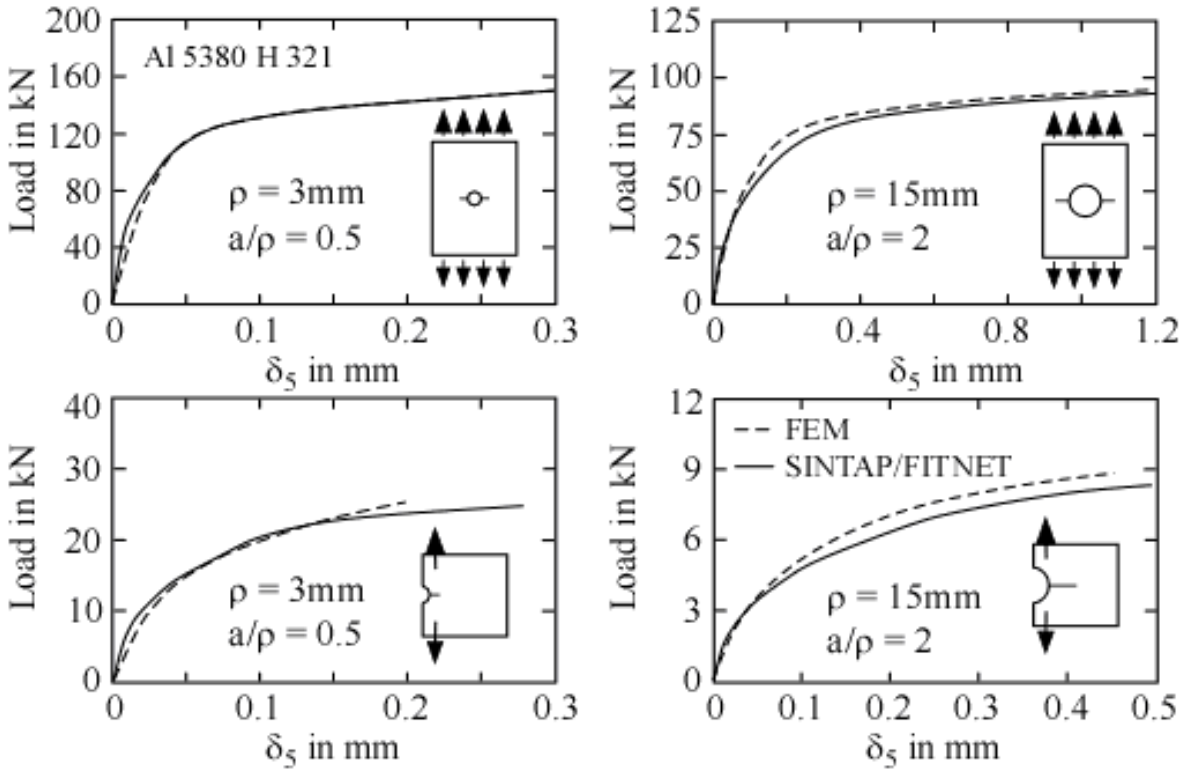

Figure 9: Comparison between the finite element and the modified SINTAP based load versus δ_5 characteristics for the aluminium alloy AL 5380 H 321, Section 4.

5. APPLICATION TO A STIFFENED PANEL

The second application refers to the curved and stiffened panel shown in **Figure 10**. It is loaded by internal pressure, i.e., the axial stress is approximately half as large as the circumferential or hoop stress.

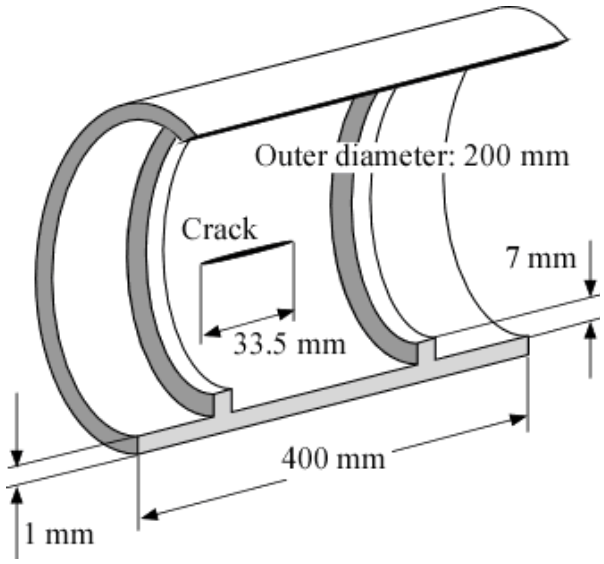

Figure 10: The panel investigated in Section 5. It is loaded by internal pressure.

Whereas the analyses in Section 4 were restricted to predicting the crack driving force, a complete failure analysis is performed for the stiffened panel. The material chosen was the aluminium alloy Al 5083 H321, the tensile properties of which have been given in Figure 6 and Table 2. The δ_5-R curves for characterising the resistance against stable crack extension are shown in **Figure 11**. Whereas the M(T)-R curves for different specimens widths (50 and 150 mm) coincide over the whole Δa range, the C(T) curves diverge earlier. The validity limit introduced in the figure, $\Delta a_{max} = 0.25\ (W\text{-}a_o)$, refers to the C(T)1000 specimen with a width of 1000 mm. The specimen thickness was 3 mm in each case. The subsequent analyses were based on the C(T)1000-R curve and alternatively on the M(T)-R curve. Both curves coincide at larger crack extensions Δa [27] but differ at small Δa values where the M(T)-R curve lies above the C(T) curves. Note, however, that the determination of the initial part of the R curve in thin-walled plates of aluminium is problematic because of pronounced crack tip tunnelling in the initial phase. That means the crack grows faster in the centre of the specimen than at its surface where Δa is optically measured. After a few millimetres the crack front tends to straighten thus making the crack length measurement at the surface less uncertain. This aspect has to be considered when evaluating the results of the assessment.

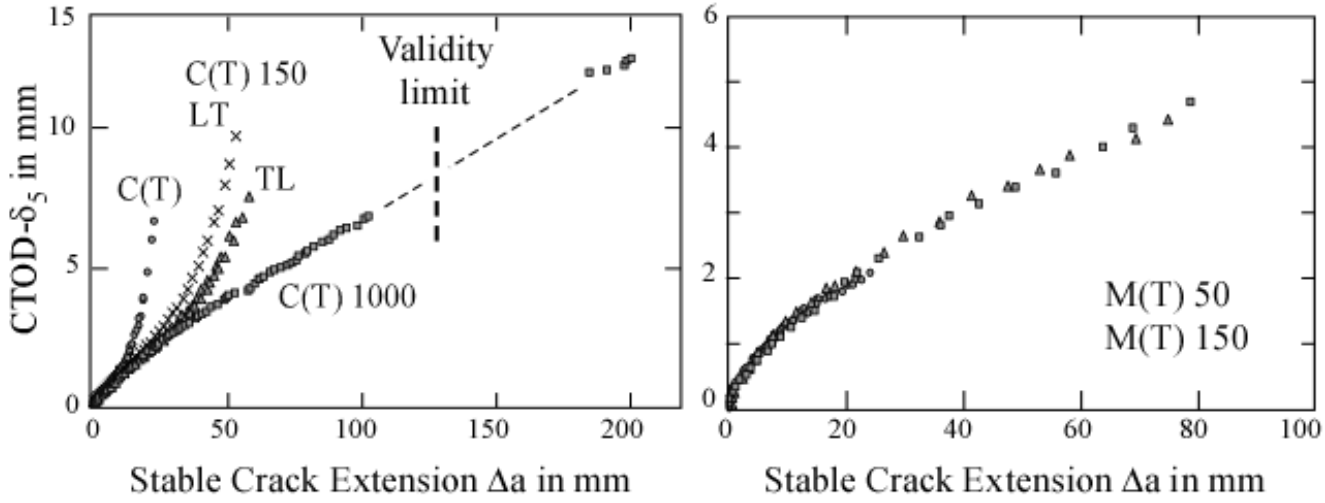

Figure 11: Fracture resistance(R)-curves of the aluminium alloy Al 5083 H321. (according to [27]).

The stress intensity factor, K, and reference load, F_Y, solutions are obtained as described in Section 3 by finite element analyses (ABAQUS [26]). The calculations were performed for large deformations using a shell model. Since ABAQUS [26] does not allow the application of line integrals for J-integral determination in shells this quantity was obtained as an energy release rate by modelling two slightly different crack lengths for each calculation. **Figure 12** shows the distribution of the hoop stress across the wall for an internal pressure of 1 MPa. The resultant stress intensity factor and F_Y values for different crack lengths are shown in **Figure 13**.

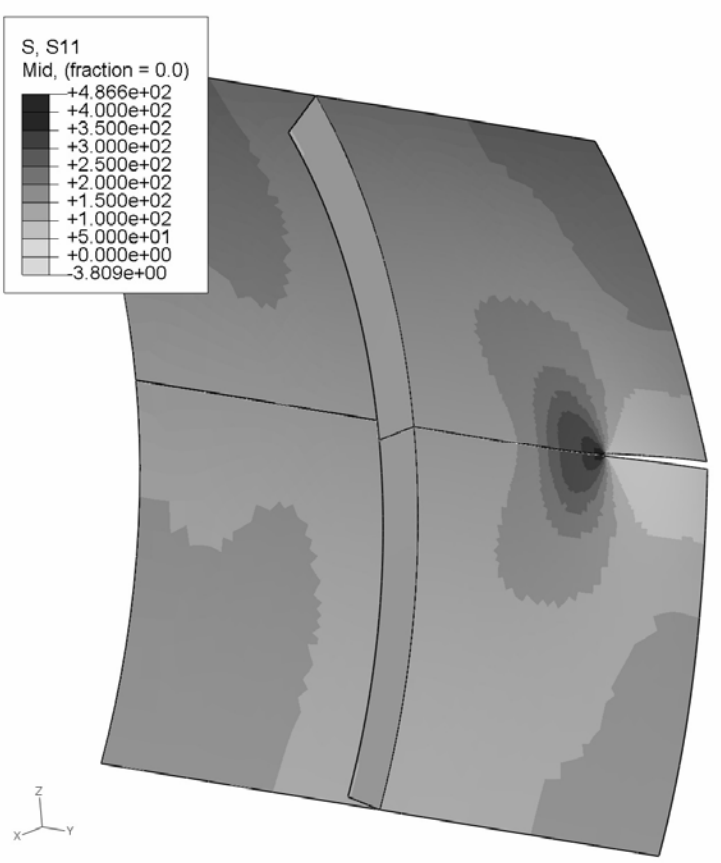

Figure 12: Finite element analysis of the loaded structure in Section 5. The legend shows the hoop stress in MPa for an internal pressure of 1 MPa.

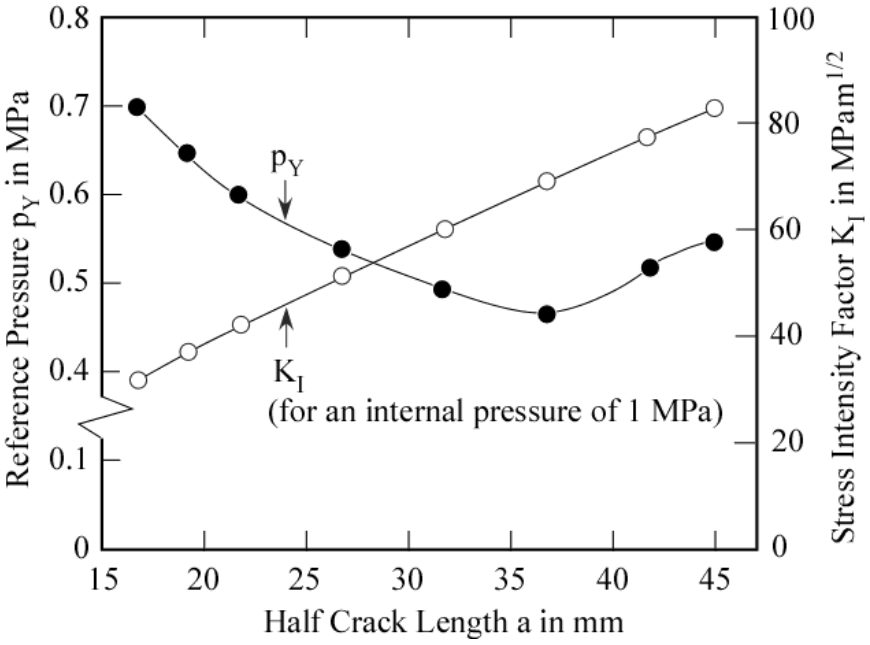

Figure 13: Mode I stress intensity factor, K_I, (for an internal pressure of 1 MPa) and reference load, F_Y, as a function of half crack length a (see Figure 10). Both K and F_Y are determined by finite element analyses, the latter by the method described in Section 3.

The determination of the load versus stable crack extension characteristics followed the scheme in Figure 3. The results are reproduced in Figure 14 where they are compared with predictions based on the crack tip opening angle (CTOA) concept [28] and a cohesive zone model. No discussion of these methods shall be provided here, see instead [29] in this issue.

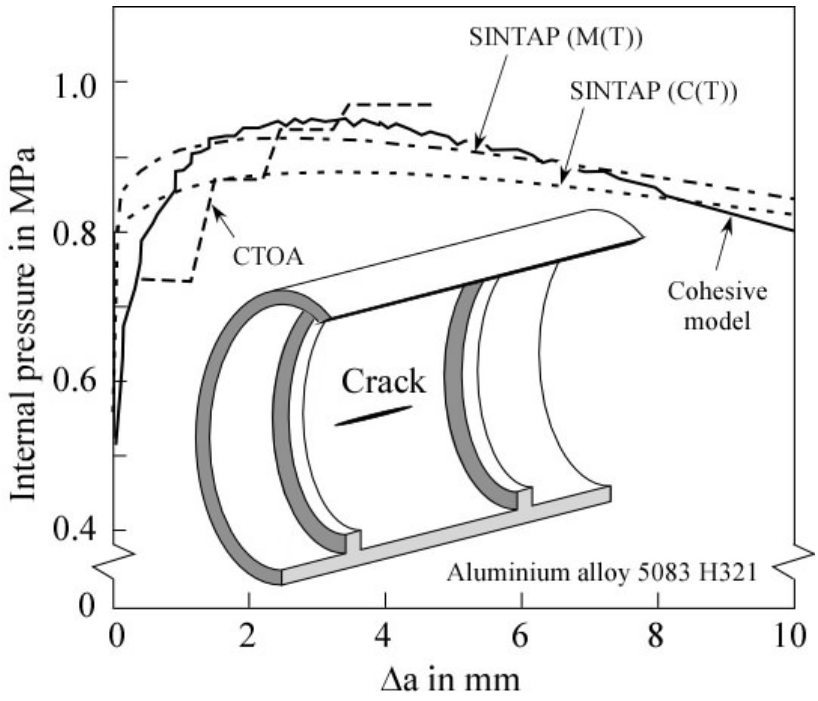

Figure 14: Comparison of the SINTA prediction of the load-Δa-characteristics with results obtained by the crack tip opening angle (CTOA) method according to [27, 28] and a cohesive zone model [29].

Two versions of the SINTAP prediction are plotted. These refer to the two different R curves applied (see above). As can be seen the resultant maximum load depends significantly on these. It was already mentioned that the R curve determination is somewhat uncertain for small Δa. In the present example the maximum load was predicted for a stable crack extension of about 3 mm based on both SINTAP and the cohesive zone model, which is fairly small. In a component geometry where the maximum load would be predicted for (moderately) larger Δa the effect would vanish because the M(T) and C(T)-R curves in Figure 11 coincide above a few millimetres crack extension.

No experimental validation of the modified SINTAP thin wall module is provided here. However the results can be compared to the results of the two other methods applied. If the M(T)-R curve is accepted to be more realistic than the C(T)-R curve for the present component geometry the maximum loads predicted by the three methods are close together. This is an indication that the method proposed here is an acceptable tool for flaw assessment.

Note that the maximum sustainable load is the target information of the assessment. In practice this would be compared with the maximum load expected in service. The crack

growth regions below and beyond this maximum load are of almost no importance for practical application. Nonetheless it has to be stated that the predictions of the different methods in these regions significantly differ. For SINTAP particularly the initial Δa region seems to be unrealistic. Again the reason could be in the initial R curve. **Figure 15** shows the typical early growth of a stable crack in a thin walled structure including crack tip tunnelling and the "flat-slant" transition of the crack orientation. Note that these effects are not distinguished in a δ_5-R curve (or J-R curve likewise). Schödel, comparing crack lengths measurements at the fracture surface (multiple specimens technique) and at the side surfaces found the latter to be 0.2 to 0.35 mm smaller in the initial phase of stable crack extension [27] which could at least partially explain the unlikely curve progression up to Δa = 2 mm in Figure 14.

In Section 2 it was required that the stable crack extension referring to the predicted maximum load in the component should not exceed the Δa range which is covered by the experimental R-curve. This condition was fulfilled. However a further requirement should be added here: the maximum load in the component should refer to a Δa equal or larger than that for which the crack front across the specimen thickness becomes approximately uniform or "stationary". For the Al 5083 H 321 used in this study this was the case beyond about Δa = 2 to 3 mm [27], **Figure 16**.

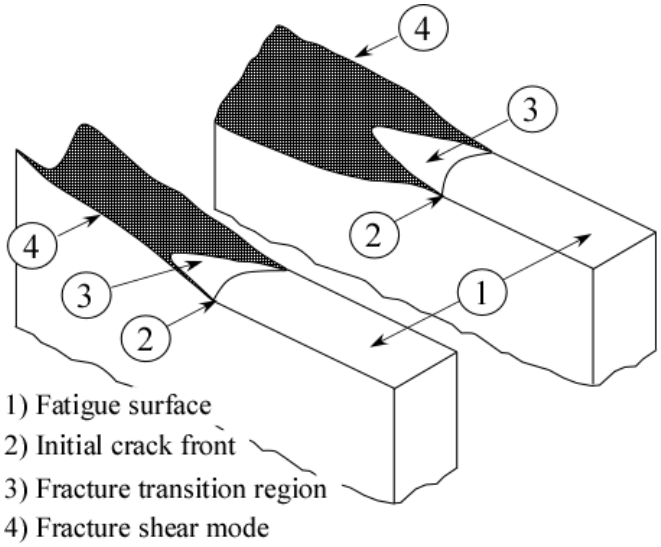

Figure 15: Early crack extension showing crack tip tunneling and "flat-slant" transition.

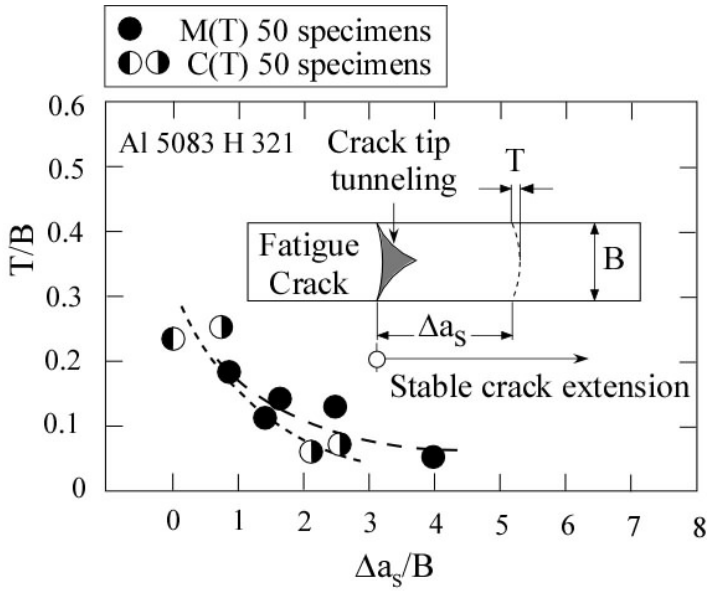

Figure 16: Crack tip tunneling and transition to "stationary" crack extension (according to [27].

6. Concluding Remarks

A definition of the limit or yield load, which the authors more generally designate as "reference load", is proposed which is based on the SINTAP Option 3 failure assessment function for an L_r value of 1. This can be determined by finite element analyses for any component geometry. This approach is then applied to two typical thin walled geometries. A set of 54 plane stress finite element simulations of notched geometries with varying notch radii and crack sizes as well as loading types (tension, combined bending and tension) and materials (a ferritic and an austenitic steel and an aluminium alloy) is used for determining reference loads and for validating the procedure, but limited to the crack driving force in the components. The second application is a curved and stiffened panel for which the maximum load the structure can sustain is predicted and compared to alternative analyses based on the crack tip opening angle (CTOA) and a cohesive zone model. The proposed methodology has been shown to be suitable tool for flaw assessment of complex thin wall structures. It is intended to complement the existing flaw assessment procedure SINTAP.

Literature:

[1] Schödel, M. and Zerbst, U. (2004): Application of the European flaw assessment procedure SINTAP to thin wall structures. Analytical assessment levels. Engng. Fracture Mech. 71, 1035-1058.

[2] Schödel, M., Zerbst, U. and Dalle Donne, C. (2006): Application of the European flaw assessment procedure SINTAP to thin wall structures subjected to biaxial and mixed mode loadings. Engng. Fracture Mech. 73, 626-642.

[3] Kocak, M., Webster, S., Janosch, J.J., Ainsworth, R.A. and Koers, R. (2006): Fitness for Service Procedure (FITNET), Final Draft 7.

[4] Zerbst, U., Schödel, M., Webster, S. and Ainsworth, R.A. (2007): Fitness-for-Service Fracture Assessment of Structures Containing Cracks. A Workbook based on the European SINTAP/FITNET Procedure. Elsevier.

[5] Schwalbe, K.-H. (1995): Introduction of δ_5 as an operational definition of the CTOD and its practical use. ASTM STP 1256, pp. 763-78. American Society for Testing and Materials.

[6] R6, Revision 4 (2000): Assessment of the Integrity of Structures Containing Defects. British Energy Generation Ltd (BEGL), Barnwood, Gloucester.

[7] Schwalbe, K.H-, Newman, J.C., Jr. and Shannon, J.L. Jr. (2005): Fracture mechanics testing on specimens with low constraint—standardization activities within ISO and ASTM. Engng. Fracture Mech. 72, 557-576.

[8] ASTM E 2472 – 06 (2007): Standard Test Method for Determination of Resistance to Stable Crack Extension under Low Constraint Conditions. Annual Book of ASDTM Standards, Vol. 03.01, 1411-1436, American Society for Testing and Materials (ASTM).

[9] Newman JC Jr, James MA, Zerbst U. A review of the CTOA/CTOD fracture criterion. Engng. Fract. Mech. 2003; 70: 371-385.

[10] Schwalbe KH and Heerens J. R-curve testing and its relevance to structural assessment. Fat. Fract. Engng. Mat. Struct. 1998; 21: 1259-1271.

[11] Zerbst, U. and Schödel, M. (2003): Bruchmechanisches Bewerten dünnwandiger Strukturen. Materialprüfung 45, pp. 519-525.

[123] FITNET [3], Annex B: Limit Load Solutions.

[13] Miller, A.G. (1988): Review of limit loads of structures containing defects. Int. J. Pressure Vessel & Piping 32, pp. 197-327.

[14] R6, Revision 4: Assessment of the Integrity of Structures Containing Defects. British Energy Generation Ltd (BEGL), Barnwood, Gloucester 2004, Chapter IV.1: Limit load solutions for homogenous components.

[15] BS 7910 (2005): Guide on Methods for Assessing the Acceptability of Flaws in Metallic Structures. British Standard Institution, London, Annex P: Calculation of reference stress.

[16] Schwalbe, K.-H., Zerbst, U., Kim, Y.-J., Brocks, W., Cornec, A., Heerens, J. and Amstutz, H. (1998): EFAM ETM 97: The ETM Method for Assessing Crack-Like Defects in Engineering Structures, GKSS Research Centre, Geesthacht, GKSS Report 98/E/6.Appendix 1: Solutions for Stress Intensity Factor, K, Yield Load, F_Y and κ.

[17] API 579 (2000): Recommended Practice for Fitness for Service. American Petroleum Institute (API), Washington, Appendix D: Compendium of Reference Stress Solutions.

[18] Zahoor, A. (1989-1991): Ductile Fracture Handbook. Novotech. Cop & EPRI, Res. Proj. 1757-69; Vol. 1: 1989, Vol. 2: 1990, Vol.: 1991.

[19] V. Kumar, M.D. German and C.F. Shih (1981): An Engineering Approach for Elastic-Plastic Fracture Analysis, General Electric Company, NP-1931, Research Project 1237-1, Topical Report.

[20] Zerbst, U., Ainsworth, R.A. and Schwalbe, K.H. (2000): Basic principles of analytical flaw assessment methods. Int. J. Press Vess. Piping, **77**, 855-67.

[21] Schwalbe, K.-H. and Zerbst, U. (2003): Crack driving force estimation methods. In: Ainsworth, R.A. and Schwalbe, K.-H. (eds.) (2003): Practical Failure Assessment Methods. Comprehensive Structural Integrity (CSI), Elesevier, Amsterdam et al., Vol. 7., Chapter 7.04, 133-76.

[22] Ainsworth, R A (1984): The assessment of defects in structures of strain hardening material, Engng Fract Mech **19**, 633-642.

[23] Kim, Y-J, Shim, D-J, Huh, N-S, Kim Y-J (2004): Approximate elastic-plastic J estimates of cylinders with off-centred circumferential through-wall cracks, Engng Fract Mech **71**, 1673-1693.

[24] Kim, YS.-J., Shim, D.-J., Choi, J.-B. and Kim, Y.-J. (2002): Approximate J estimates for tension-loaded plates with semi-elliptical surface cracks. Engng. Fracture Mech. 69, pp. 1447-1463.

[25] Lei, Y. (2004): J-integral and limit load analysis of semi-elliptical surface cracks in plates under combined tension and bending. Int. J. Pressure Vessel and Piping 81, pp. 43-56.

[26] ABAQUS, Version 6. (2006), ABAQUS Inc., Providence RI.

[27] Schödel, M. (2006): Bruchmechanische Untersuchungen der Rissöffnung bei stabilem Risswachstum in dünnem Blech aus Al 5083. PhD Thesis, TU Hamburg, GKSS Report 2006/6.

[28] Schödel, M., Scheider, I., Iberer, T. and Rother, K. (2005): Residual strength of thin-walled structures based on the CTOA approach of ANSYS. 23rd CAD-FEM Users Meeting.

[29] Zerbst**,** U., Heinimann, M., Dalle Donne, C. and Steglich, D. (2008): Fracture and damage mechanics modelling of thin-walled structures – an overview. Engng. Fracture Mech. This issue, Xxxxxxxxxxx

Nomenclature:

a	Crack length
a_o	Initial crack length prior to stable crack extension
B	Specimen thickness
E	Modulus of elasticity
E’	Modulus of elasticity for constraint conditions (plane stress: E’ = E; plane strain: E’ = E/(1-ν^2)
F	Applied load (general term and tensile force)
F_Y	Limit or yield load (here designated as reference load)

$f(L_r)$	Failure assessment curve function in R6 and SINTAP
J	J-integral
J_e	Elastic component of the J-integral
J_{ep}	Elastic-plastic J-integral
K	Linear elastic stress intensity factor
K_I	Mode I stress intensity factor
L_r	Ratio of applied load to limit or yield load (here designated as reference load)
L_r^{max}	Maximum allowable value of L_r
m	Constraint factor (Eqn. 2)
R_{eL}	Elastic stress limit of steels with a Lüders plateau
$R_{p0.2}$	Yield strength at 0.2% plastic strain
R_m	Tensile strength
W	Specimen width
T	Measure of crack front curvature (Figure 16)
β	Notch factor (Eqns. 10 and 11; Tables 3 and 4)
δ_5	CTOD defined for a gauge length of 5 mm
δ_{5e}	Elastic CTOD-δ_5
δ_{5ep}	Elastic-plastic CTOD-δ_5
Δa	Stable crack extension
Δa_{max}	Validity criterion for δ_5-R curves, maximum Δa
Δa_s	Stable crack extension at specimen surface (Figure 16)
ε_{ref}	Reference strain, Eqn. (4), Fig. 2
ρ	Notch radius
σ_{ref}	Reference stress, Eqn. (4), Fig. 2
σ_Y	Yield strength, general (R_{eL} or $R_{p0.2}$)

Abbreviations

CTOA	Crack tip opening angle
CTOD	Crack tip opening displacement
C(T)	Compact tension specimen
FITNET	European Fitness for Service Network
M(T)	Middle cracked tension specimen
R curve	Crack (extension) resistance curve
R6	R6 routine of British Energy.
SINTAP	Structural Integrity Assessment Procedure for European Industry